Yuzuncu Yil University Journal of the Institute of Natural & Applied Sciences

https://dergipark.org.tr/en/pub/yyufbed

Research Article

A Fluorine-Free Polyethersulfone Composite Membranes Doped with Waste Newspaper-Derived Cellulose for PEMFCs

Nisa Doğa ERDEMİR [1], Çağla CAN [1], Yavuz YAĞIZATLI [1*]

[1]Department of Chemical Engineering, Gazi University, 06570, Ankara, Türkiye

*Corresponding author e-mail: yavuzyagizatli@gazi.edu.tr

Abstract: Waste newspapers were converted into high-value cellulose and used as a bio-based additive in the production of polyethersulfone (PES) composite membranes. It was aimed to improve proton transport while maintaining mechanical stability. Cellulose was obtained from the newspaper through successive deinking, cleaning and hydrolysis steps. Then incorporated into PES at weight percentages of 1%, 5%, and 10% via solution casting. Fourier transform infrared (FTIR) and X-ray diffraction (XRD) confirm that the cellulose backbone is preserved and the PES structure is maintained, with no evidence of new covalent bond formation, indicating a physical mixture where secondary interactions are dominant. Thermal analysis reveals that although cellulose addition alters the thermal degradation behavior of the membrane, the same mass conservation value is achieved at 800°C. Hydration-related properties were temperature-dependent and not monotonic with loading. The highest water uptake was observed with 5% cellulose (water uptake capacity: 7.91 at 25°C and 9.97 at 80°C), whereas 10% cellulose exhibited lower water uptake (water uptake capacity: 2.16 at 25°C; 3.09 at 80°C), which is due to morphology and distribution effects. Mechanical tests showed that the tensile strength increased from 48.3 MPa to 58.7 MPa with 5% cellulose doped. Electrochemical impedance spectroscopy determined that the resistance of the PES-%10 Cellulose membrane decreased by %58.7 compared to pristine PES, and the proton conductivity increased from 2.73 to 14.8 mS cm^{-1}. Overall, waste-derived cellulose effectively improved proton transport in PES membranes, and performance depended on the balance between hydrophilic pathway coupling and composite structure.

Keywords: PEMFC, Membrane, Cellulose, PES, Composite

PEMFC'ler için Atık Gazeteden Elde Edilen Selüloz ile Katkılanmış Flor İçermeyen Polieter Sülfon Kompozit Membranlar

Özet: Atık gazeteler, yüksek katma değerli selüloza dönüştürülmüş ve polietersülfon (PES) kompozit membranların sentezinde biyobazlı bir katkı maddesi olarak kullanılmıştır. Bu çalışmada, mekanik kararlılık korunurken proton iletkenliğinin iyileştirilmesi hedeflenmiştir. Selüloz, gazete atıklarından mürekkep giderme, temizleme ve hidroliz adımlarıyla elde edilmiştir. Elde edilen selüloz daha sonra çözelti döküm yöntemiyle ağırlıkça %1, %5 ve %10 oranlarında PES matrise dâhil edilmiştir. Fourier dönüşümlü kızılötesi spektroskopisi (FTIR) ve X-ışını kırınımı (XRD) analizlerinden, selüloz ve PES yapısının korunduğu belirlenmiştir. Ayrıca yeni kovalent bağ oluşumuna dair bir bulgu olmadığı doğrulamış, dolayısıyla ikincil etkileşimlerin baskın olduğu fiziksel bir karışım yapısına ait olduğu belirlenmiştir. Termal analizler, selüloz ilavesinin membranın termal bozunma davranışını değiştirmesine karşın 800°C'de aynı kütle korunumu değerine ulaşıldığını göstermiştir. Hidratasyonla ilişkili özellikler sıcaklığa bağlı olup katkı oranı ile paralel bir değişim sergilememiştir. En yüksek su tutma kapasitesi, %5 selüloz içeren membranda gözlenmiş (su alma kapasitesi: 25°C'de 7.91 ve 80°C'de 9.97) iken, %10 selüloz içeren membran daha düşük su alma değerleri göstermiştir (su alma kapasitesi: 25°C'de 2.16;

Received Date:28.10.2025
Accepted Date: 19.01.2026

How to cited: Erdemir, N., D., Can, Ç., Yağızatlı Y. (2026). A Fluorine-Free Polyethersulfone Composite Membranes Doped with Waste Newspaper-Derived Cellulose for PEMFCs. *Yuzuncu Yil University Journal of the Institute of Natural and Applied Sciences,, 31*, 141-159. https://doi.org/10.53433/yyufbed.1858435

80ºC'de 3.09). Bu durum morfoloji ve dağılım etkilerine atfedilmiştir. Mekanik testler, çekme dayanımının %5 selüloz katkısıyla 48.3 MPa'dan 58.7 MPa'a yükseldiğini ortaya koymuştur. Elektrokimyasal empedans spektroskopisi, PES-%10 Selüloz membranının direncinin saf PES'e kıyasla %58,7 azaldığını ve proton iletkenliğinin 2.73 mS cm^{-1}'ten 14.8 mS cm^{-1}'e arttığını belirlemiştir. Sonuç olarak, atık kaynaklı selüloz PES membranlarda proton taşınımını etkin biçimde iyileştirmiş, performansın ise hidrofilik yolakların bağlantılanması ile kompozit mikro yapı arasındaki dengeye bağlı olduğu görülmüştür.

Anahtar Kelimeler: PDMYP, Membran, Selüloz, PES, Kompozit

1. Introduction

At present, global energy demand is largely met by fossil fuels such as oil, coal, and natural gas. However, the finite nature of these resources, combined with rapidly increasing consumption, indicates that they will be unable to satisfy future energy needs. In addition, the combustion of fossil fuels releases substantial amounts of carbon dioxide (CO_2) and other greenhouse gases, leading to serious environmental problems and accelerating climate change (Nong et al., 2021; S. Thangarasu & T.-H. Oh, 2022). These limitations have intensified the transition towards clean, sustainable, and renewable energy sources.

For a few years, hydrogen energy has gained importance as a clean energy carrier. Hydrogen has approximately three times higher chemical energy per unit mass compared to gasoline or diesel (Council, 2006; Hossain Bhuiyan & Siddique, 2025). Hydrogen can be produced cleanly from renewable sources through methods (Yörük et al., 2025). A conspicuous application of hydrogen energy technology is fuel cells. Fuel cells are electrochemical devices that can convert the chemical energy of fuels, such as hydrogen, directly into electrical energy with high efficiency.

Proton exchange membrane fuel cells (PEMFCs), a type of fuel cell, have attracted the most attention due to their ability to operate at relatively low temperatures and use hydrogen directly as fuel (Phogat et al., 2025). PEMFCs are currently the subject of extensive study to supply clean energy for various applications, ranging from portable devices to transportation. PEMFC is of great importance as a clean energy conversion technology, under suitable conditions, it can generate electricity by producing only harmless products. The proton exchange membrane (PEM), which permits proton transfer, is one of the most essential parts of a PEMFC. Protons created as a result of fuel oxidation can be carried towards the cathode via a membrane that divides the anode and cathode compartments, keeping fuel and oxidant from mixing (Spiridigliozzi, 2018). The choice and characteristics of the membrane directly impact the fuel cell's performance. High proton conductivity, sufficient water uptake to maintain conductivity, low permeability to fuel and oxygen, as well as good mechanical, thermal, and chemical stability are essential requirements for an effective membrane (Tellez-Cruz et al., 2021). Membranes that meet these criteria play a critical role in determining the efficiency and lifespan of a fuel cell.

Nafion is the most commonly used commercial membrane in PEMFC. It is a perfluorosulfonic acid (PFSA) polymer that has attracted significant interest due to its superior proton conductivity, as well as its excellent chemical and thermal stability (Daud et al., 2015). However, Nafion also has significant drawbacks. The production cost is notably elevated, and the high conductivity is preserved solely in adequately humid environments. Under low relative humidity or at elevated temperatures, its proton conductivity decreases markedly. In addition, Nafion shows relatively high permeability to fuels such as hydrogen and alcohols, which can cause fuel crossover and loss of efficiency. Due to its fully fluorinated polymer backbone, Nafion is also non-biodegradable, which raises concerns about waste management and limits its environmental sustainability at the end of its service life (Di Virgilio et al., 2023; Teixeira et al., 2023). For these reasons, there is a need to develop an alternative membrane that can replace Nafion. In the search for new membranes, both chemical modifications of synthetic polymers and composite membrane approaches are attracting attention. Different polymer matrix, such as polyvinyl alcohol (PVA), sulfonated polyether ether ketone (SPEEK), polyvinylidene difluoride (PVDF), and polyether sulfone (PES), are investigated as alternatives to Nafion (Zhou et al., 2019; Golubenko et al., 2022; Justin Jose Sheela et al., 2023; Teixeira et al., 2025). Among these, PES offers high thermal/mechanical stability, good chemical resistance to oxidizing environments, and easy film formation thanks to its aromatic backbone (Wang et al., 2015). Furthermore, PES is fluorine free, cheap,

and commercially readily available makes it stand out as a more economical and environmentally sustainable membrane matrix compared to Nafion (Sanchez et al., 2009).

One alternative membrane development strategy is to create composite membranes by adding additives to existing polymer membranes. Suitable additives added to the membrane matrix help to overcome the disadvantages of the polymer and improve its desired properties. The most commonly used inorganic additives are SiO_2, TiO_2, ZrO_2, WO_3, nanoclay, and carbon-based nanomaterials (Treekamol et al., 2014; Yagizatli et al., 2020; Selim et al., 2022; Woo et al., 2022; Madheswaran et al., 2023; Poongan et al., 2023). These additives positively impact fuel cell performance by performing various functions, such as increasing the proton conductivity of the membrane, creating a gas-permeability barrier, and enhancing mechanical strength. Biopolymer additives, especially cellulose and its derivatives, are attracting significant interest in fuel cell membranes (Samaniego & Espiritu, 2022; Thangarasu & Oh, 2022). Cellulose is a naturally occurring polysaccharide rich in hydroxyl functional groups and is the most common biopolymer in the world (Seddiqi et al., 2021). Owing to its renewable, low-cost nature, cellulose based materials play an important role in the design of sustainable proton-conducting membranes. When incorporated into a polymer matrix, cellulose based additives can improve the mechanical strength of the membrane, and serve as carriers for additional functional groups that further enhance proton transport and interfacial properties.

Herein, cellulose doped PES membranes were synthesized and characterized as potential candidate membranes for PEMFC related applications. For waste management and production of value added products, cellulose was obtained from waste newspaper. The obtained cellulose was then characterized using scanning electron microscopy coupled with energy-dispersive X-ray spectroscopy (SEM-EDX), Fourier transform infrared (FTIR) spectroscopy, particle size analysis, and X-ray diffraction (XRD). Subsequently, PES membranes containing 1, 5, and 10 wt% cellulose were synthesized by the solution-casting method. Water uptake, swelling behavior, thickness change, ion-exchange capacity, mechanical strength, and impedance analyses were performed for the synthesized membranes. In addition, the membranes were characterized by FTIR, XRD, thermogravimetric analysis-differential thermal analysis (TGA-DTA), and SEM.

2. Material and Methods

For the synthesis of cellulose from waste newspaper, sodium hydroxide (NaOH, >99%, pellet, Sigma), hydrogen peroxide (H_2O_2, 35%, Sigma), sodium metasilicate (Na_2SiO_3, ≥98%, Sigma), and sulfuric acid (H_2SO_4, ≥97%, Sigma) were used. For membrane synthesis, polyethersulfone (PES, 3 mm nominal granules, Merck) was used as the main polymer and dimethyl sulfoxide (DMSO, $(CH_3)_2SO$, ≥99.9%, Merck) was used as the solvent.

2.1. Cellulose synthesis from waste newspaper

The synthesis of cellulose from waste newspaper was carried out in four main stages: dye removal, chemical hydrolysis, cellulose structure formation, and drying. In the first stage, 20 g of waste newspaper cut into small pieces was treated with 100 mL of 1.5 M NaOH, 100 mL of 3 M H_2O_2, and 100 mL of 1 M Na_2SiO_3 at 50°C under stirring at 1200 rpm for 3 h, corresponding to a solid to liquid ratio of 1:15 (g:mL). This process removed impurities such as lignin, hemicellulose, and ink, freeing the cellulose fibers. The resulting pulp was filtered, washed at least 3 times with deionized water until near-neutral conditions were reached, and then dried at room temperature. In the second stage, it was subjected to chemical hydrolysis by stirring in a 2 M H_2SO_4 solution at 50°C for six hours, followed by washing with pure water to remove it from the acidic environment until the pH was neutral. This process resulted in the further separation of the structure into smaller sizes. In the third stage, the neutralized sample was processed in an ultrasonic homogenizer at 50% amplitude for 15 minutes to achieve a more homogeneous structure. The resulting filtrate was subjected to solid-liquid separation by centrifugation, and the remaining suspension liquid phase was dried to obtain the structure. This method ensured the removal of water from the medium without disrupting the structural integrity.

2.2. Cellulose doped PES membrane synthesis

Solution casting method was applied in cellulose doped (with 1%, 5%, and 10% weight ratios) PES membrane synthesis. Firstly, PES polymer and prepared cellulose were dried in an oven for 24 hours to remove moisture. Then, a homogeneous polymer solution was prepared by dissolving the PES polymer in DMSO solvent at 70ºC. On the other side, cellulose was homogeneously dispersed in DMSO solvent using ultrasonication and magnetic stirring. The prepared cellulose solutions were added to the PES solution and homogenized using magnetic stirring for 48 hours. At the end of this stirring period, the cellulose was evenly distributed in the polymer matrix without forming agglomerations. The resulting homogeneous mixture was poured into a petri dish, and the solvent removal process was carried out in stages. In the first stage, the process was continued at 40ºC for 24 hours, and in the second stage, at 60ºC until the solvent completely evaporated and the membrane was completely dry. The thicknesses of the synthesized membranes were obtained as 67.4±2.9, 72±3.35, 85±3.11, and 98±3.45, respectively, with increasing cellulose ratios from pristine PES.

2.3. Characterization studies

FTIR analyses were conducted using a Bruker Vertex brand FTIR spectrophotometer with an ATR measuring apparatus and a DT-GS detector in the 400-4000 cm^{-1} wavelength range to determine the bonds and structural properties formed in the synthesized membrane structure.

XRD analyses were performed to determine the amorphous/crystalline phases, crystal size, and synthesis success of the synthesized cellulose and membranes. XRD analyses were recorded using a Rigaku D/MAX 2200 instrument.

Particle size analysis was performed using a Malvern Zetasizer, and the results are reported as a DLS-based intensity-weighted hydrodynamic size distribution.

SEM analysis was performed using a ZEISS Sigma 300 instrument to examine the surface morphology of cellulose and membrane structures. The structure on the surface was visualized at specific magnifications using the instrument.

To determine the thermal stability of the pristine membrane and doped-membrane, TGA-DTA analysis was performed using a Perkin Elmer Pyris 1 Thermogravimetric Analyzer at temperatures between 25-800ºC and a heating rate of 10ºC/min.

The synthesized membranes were tested for fuel cell applications using water uptake capacity (WU_c), swelling properties (S_p), dimensional change (D_c), dynamic mechanical analysis (DMA), ion exchange capacity (IEC), and impedance analysis (EIS). For WU_c, S_p, and D_c tests, membranes were cut into 1x1 cm pieces and dried in an oven before testing. First, the dry weight, thickness, and dimensions of the membranes were determined. Then, after the membranes were kept in pure water at temperatures of 25ºC and 80ºC for 24 hours, the excess water on the surface was removed, and the wet weight, thickness, and dimensions were measured to determine the WU_c (1), S_p (2), and D_c properties (3) of the membrane. All WU_C, S_P, and D_C measurements were performed in 3 independent replicates, and the results are reported as mean standard deviation.

$$WU_c = \frac{wet\ weight - dry\ weight}{dry\ weight}\ x\ 100 \quad (1)$$

$$S_p = \frac{wet\ thickness - dry\ thickness}{dry\ thickness}\ x\ 100 \quad (2)$$

$$D_c = \frac{wet\ area - dry\ area}{dry\ area}\ x\ 100 \quad (3)$$

The mechanical strength of the membranes was determined by DMA. DMA was performed using a Shimadzu brand mechanical analyzer. All membranes were cut to dimensions of 2 mm x 10 mm, and tensile strength tests were conducted at room temperature at a tensile speed of 3 mm/min. To make a preliminary assessment of the titration based ion-exchange behavior of the membrane matrix after acid

pretreatment, IEC measurements of the synthesized membranes were carried out. Before the measurements, the membranes were cut to the same dimensions and the dry mass of each sample was determined by precision balance. Then, the membranes were converted to proton form by being kept in H_2SO_4 solution for 24 hours and then in pure water for the following 24 hours. The protonated membranes were then placed in 0.1 M NaCl solution for 48 hours. At the end of the period, the membranes were removed from the solution, and the IEC value (4) of each membrane was determined by titration with 0.01 M NaOH. IEC measurements were performed in 3 independent replicates, and the results are reported as mean standard deviation.

$$IEC\ (meq\ g^{-1}) = \frac{consumed\ titrant\ x\ titrant\ molarity}{dry\ membrane\ weight} \quad (4)$$

The proton conductivity of the membranes (5) was determined by EIS measurements using a PalmSens potentiostat and a BT-112 conduction cell. Before the measurements, the membranes were cut to the appropriate dimensions for the BT-112 conduction cell and protonated. After protonating, EIS measurements were performed in a 0.05 M H_2SO_4 media in the frequency range of 10^5-0.1 Hz.

$$Proton\ Conductivity\ (mS\ cm^{-1}) = \frac{distance\ between\ electrodes}{resistance\ x\ width\ x\ thickness} \quad (5)$$

3. Results

Comparative FTIR spectra of waste newspaper - cellulose and pristine PES - cellulose doped PES membrane are given in Figure 1, obtained from FTIR analysis performed to determine the change in structural bonds and assess synthesis success.

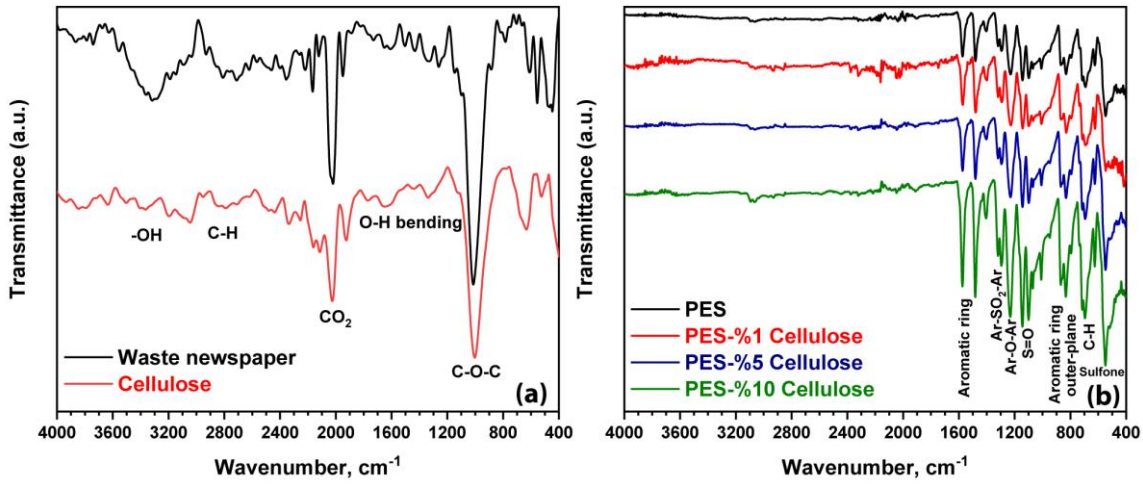

Figure 1. Comparative FTIR spectra of a) cellulose and waste newsprint and b) pristine PES and cellulose doped PES membranes.

The FTIR spectra of waste newspaper and the cellulose derived from it (Figure 1a) show that both characteristic bands belonging to the cellulosic backbone are present. However, additional bands originating from fillers/inorganic additives and partly lignocellulosic impurities are more prominent in newspaper. In the FTIR of cellulose, broad O-H stretching typically ranges from 3700–3000 cm^{-1}, C-H stretching around ~2900 cm^{-1}, CH_2 deformation around 1430-1420 cm^{-1}, and C-O-C/C-O vibrations in the 1200-900 cm^{-1} fingerprint region are dominant (Kumar et al., 2014; Plermjai et al., 2019; Chambre & Dochia, 2021; Vârban et al., 2021). In addition to the cellulose bands, bands originating from carbonate-based fillers and/or clay minerals were observed in the newspaper spectrum. For waste newspaper, distinct bands around 885 cm^{-1} and 704 cm^{-1} are consistent with the characteristic vibrations of the carbonate group (Huang & Kerr, 1960). Similarly, it has been reported that mineral additives used in newspaper production give diagnostic bands in FTIR around 3695 and 3620 cm^{-1} (-OH stretching)

and around 1000-1030, 910, 540 and 470 cm^{-1} (Luhar et al., 2021). Such additives increase the intensities, especially in the low wavenumber region. The main change expected after cellulose extraction is the weakening of inorganic filler bands and the cellulose fingerprint region becoming more cellulose-dominant. While the position of the bands corresponding to the carbonate region in the cellulose FTIR spectrum is preserved, the relative decrease/change in band intensities indicates that the washing-treatment steps are effective in removing mineral additives. Furthermore, the carbonyl band of approximately 1730 cm^{-1} in waste newsprint is considered a critical indicator of paper/cellulose chemistry in the literature (Tintner et al., 2018). Studies monitoring newsprint aging using FTIR have reported that the band/pit range of 1740-1690 cm^{-1} is associated with carbonyl/carboxyl groups and provides a sensitive indicator of cellulose chemical modification (Pagacz et al., 2020).

In the FTIR spectrum of pristine PES membrane (Figure 1b), aromatic skeleton and sulfone/ether functional bands are dominant. For pristine PES, the main bands are approximately 1573.6 cm^{-1} and 1481 cm^{-1} (aromatic ring vibrations), 1295 cm^{-1} (Ar-SO_2-Ar associated region), 1228 cm^{-1} (Ar-O-Ar/ether bond), 1143 cm^{-1} and 1099.2 cm^{-1} (SO_2 group associated vibrations) and 831 cm^{-1} (aromatic ring outer-plane vibrations) (Sandoval-Olvera et al., 2017; Koloti et al., 2018; He et al., 2019). As cellulose addition (1%, 5%, 10%) increases, the positions of the characteristic PES bands are preserved, and no new bands, not belonging to the PES backbone, appear in the spectrum. This suggests that cellulose forms the composite structure through physical mixing/dispersion rather than covalent bonding via chemical bonds to the PES matrix. Similarly, the absence of "new band formation" and the predominantly physical/hydrogen bond-based interaction in PES-cellulose-based composites are frequently reported in the literature. However, due to the -OH-rich structure of cellulose, it has been determined that the O-H band in the 3600-3000 cm^{-1} range in composite membranes increases as the cellulose content increases. Furthermore, in composites, the overlap of C-O-C/C-O vibrations of cellulose with PES bands in the 1200-900 cm^{-1} fingerprint region indicates that cellulose addition is not seen as a separate new peak, but rather as changes in band intensity/shape in this region (Qu et al., 2010; Etale et al., 2023). Similarly, cellulose gives bands sensitive to C-O vibrations around 1030 cm^{-1} and glycosidic bonds around 900 cm^{-1}, while PES carries bands associated with sulfone/ether linkages in the same region. Therefore, the change in intensities in the 1200-900 cm^{-1} band region as the cellulose content increases in the spectrum can be considered an indirect indication that cellulose has been successfully transported into the matrix. FTIR shows that the characteristic chemical backbone of PES is preserved in composites, and that the -OH induced top region behavior and fingerprint region profile change as the cellulose content increases. These findings support the formation of composite membranes through hydrogen bonding/secondary interactions and physical dispersion, rather than through the chemical formation of new bonds by cellulose within PES.

To determine the crystal structures of cellulose, pristine PES, and 10% cellulose-doped PES membranes and to ascertain the removal of impurities, XRD analyses were performed, and comparative XRD patterns are given in Figure 2.

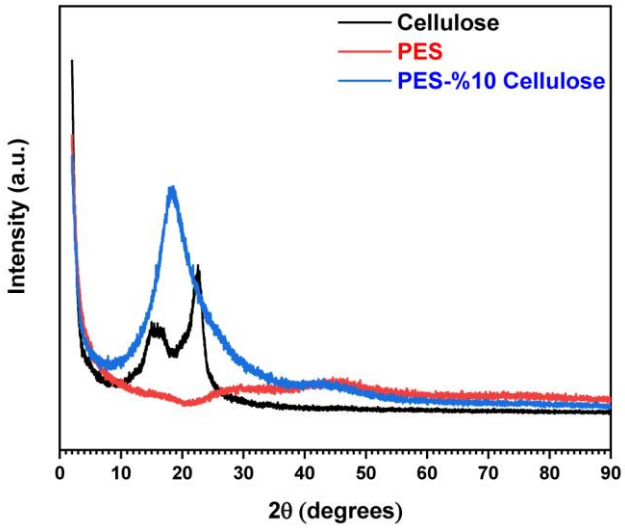

Figure 2. XRD patterns of pristine PES, cellulose, and cellulose-doped PES membrane.

The XRD spectrum of cellulose exhibits diffraction peaks characteristic of cellulose. Strong reflections around 2Θ ~14.8°, 16.4°, and 22.6° are characteristic peaks of cellulose (Oprică et al., 2023). This pattern shows that the cellulosic structure is preserved in the material obtained from waste newspaper. In terms of cellulose purity, it is reported that the strongest reflections with Cu Kα are mainly around ~29.4° (104), and additional peaks are given in the range of ~39-49°, especially for crystalline inorganic filler phases and especially for calcite ($CaCO_3$), which is a common filler in the paper industry (Wang et al., 2018). The absence of such prominent calcite reflections in cellulose indicates that the crystalline filler/ash content has been largely removed. In the pristine PES, a broad "halo" character is observed instead of distinct sharp Bragg peaks, indicating that PES is mostly amorphous (Oh et al., 2020; Zhang et al., 2020). In the PES pattern with 10% cellulose additive, while the amorphous halo of PES is preserved, the reflections of cellulose (especially around 15-17° and 22-23°) are observed to overlap the halo in a shoulder. This indicates that the cellulose is present in the composite without completely losing its crystalline domains, but the peak intensity weakens and widens within the polymer matrix, resulting in a decrease in crystalline domain size and arrangement.

SEM analysis was performed to determine the surface morphologies of the membranes. Figure 3 demonstrate SEM images of pristine PES and %10 cellulose doped PES membranes at different magnifications. Figure 3e also shows the results of the cellulose size analysis.

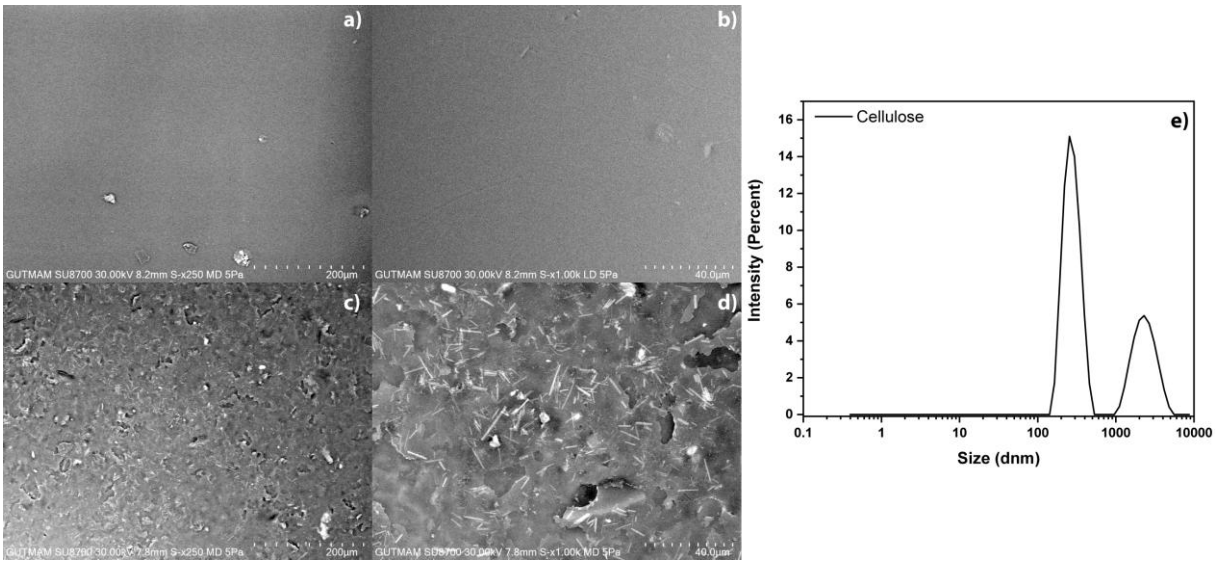

Figure 3. SEM images of a-b) pristine PES and c-d) PES-%10 Cellulose, e) cellulose size analysis.

Surface SEM images of the pristine PES membrane (Figure 3a, b) show a homogeneous and relatively smooth top surface character. Skin layer formation and consequently a denser top layer are commonly reported in the literature for hydrophobic polymer membranes similar to PES (Yang et al., 2020; Nazri et al., 2021). This was attributed to solvent evaporation induced densification of the polymer-rich surface layer during film formation. Indeed, PES itself generally exhibits more limited hydrophilic interactions in its pristine state due to its amorphous and hydrophobic character. This can be associated with a relatively more closed texture on the surface (Nazri et al., 2021). On the surface of the PES membrane with 10% cellulose doped (Figure 3c, d), an increase in surface roughness, a more pronounced heterogeneity, and the formation of structural irregularities along with cellulose derived fibril structures in some areas were observed compared to pristine PES (Acarer Arat, 2026). This is consistent with the incorporation of hydrophilic cellulose into the PES matrix. The hydrophilic -OH groups of cellulose likely influenced the evaporation induced structural development of the casting solution, resulting in significant differences in surface texture. In the literature, higher roughness, porosity, and hydrophilicity have been reported, especially in composite membranes prepared with the addition of crystalline cellulose, compared to pristine PES. These changes may be associated with the effect of cellulose on surface roughness, local heterogeneity, and structural organization during membrane formation (Adeniyi et al., 2023). The particle size distribution of cellulose (Figure 3e) shows

that it exhibits a bimodal character. It was determined to be a material with a distribution of 277.5 nm (67.4%) and 2.4 µm (32.6%), with an average diameter of 366.1 nm.

TGA-DTA was performed to determine the thermal properties of pristine PES and cellulose-doped PES membranes, and their thermograms are given comparatively in Figure 4. The thermal degradation behavior of pristine PES and PES-%10 Cellulose membranes generally exhibits a major two-stage degradation profile. For pristine PES, the temperature at which it loses 5% of its initial mass is T_5% ~ 252.6°C and the temperature at which it loses 10% of its initial mass is T_{10}% ~ 304.2°C, while for PES-%10 Cellulose, these values shift to T_5% ~ 244.5°C and T_{10}% ~ 295.7°C. This decrease is due to the volatile component of the cellulose additive in the low/medium temperature region of the composite (Pervez et al., 2022; Jahani et al., 2023).

In the low-temperature region, the composite membrane is observed to lose significantly more weight compared to pristine PES. In the 30-200°C range, pristine PES shows a loss of approximately 0.50%, while PES-10% Cellulose shows a loss of approximately 2.30%. This behavior is consistent with cellulose's ability to retain more moisture due to its hydroxyl rich structure and the increased solvent retention in the membrane after casting and solvent evaporation. It has been determined that the initial loss at low temperatures in cellulosic systems is predominantly due to physically adsorbed water, while residual solvent effects can be observed in membrane polymers within a similar range (Nurazzi et al., 2021; Jahani et al., 2023).

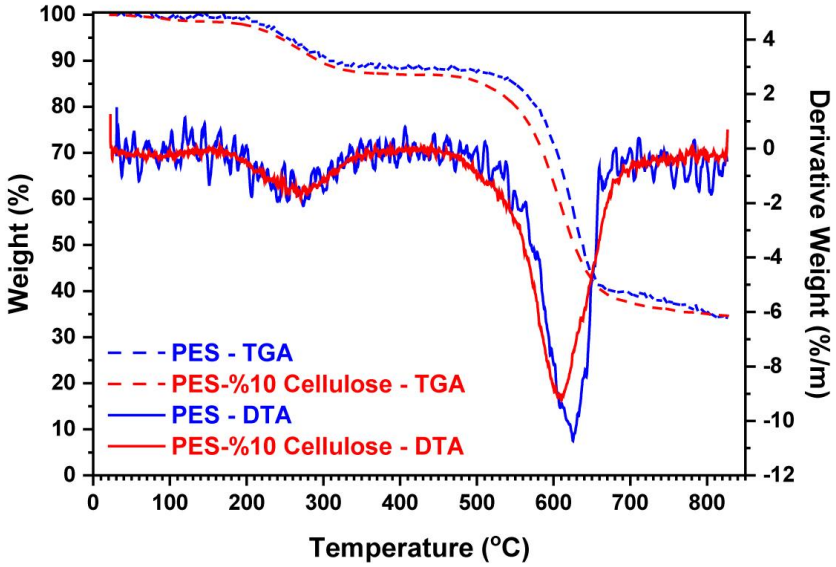

Figure 4. TGA-DTA thermogram of pristine PES and PES-%10 Cellulose.

The mid-temperature region (~200-350°C) continues with a gradual weight reduction in both membranes, and a peak corresponding to this region occurs in the DTG (DTG minimum in pristine PES ~273.6°C, in the composite ~270.2°C). This range may partly correspond to the continued release of residual DMSO retained in the membranes after solvent evaporation-based casting; in the composite membrane, it may also overlap with the onset of cellulose degradation. Thermal degradation of cellulose is reported to begin around 250-260°C, and the main degradation events in the DTG are concentrated in the 260-370°C band (Rantuch & Chrebet, 2014; Nurazzi et al., 2021). Therefore, the behavior observed in the 200-350°C band in the composite is the cumulative effect of residual solvent and the early degradation contribution of cellulose.

The high-temperature region (~500-700°C) constitutes the main degradation step for each membrane. According to DTG, the temperature at which the main weight loss rate reaches its maximum was found to be T_{max} ~ 625.8°C for pristine PES and T_{max} ~ 609.3°C for PES-10% Cellulose. Furthermore, with the DTG threshold approach, the onset of main degradation shifts to approximately 516°C in pristine PES and around 500°C in composites. This result indicates that the addition of cellulose shifts the main degradation event to a slightly lower temperature. In the literature, it has been shown that in aromatic sulfone-based polymers similar to PES, the main degradation is mostly reported in the

~ 510-600ºC range in DTG, and T_{max} can decrease depending on the type of additive (Ahmad et al., 2018; Dattilo et al., 2020). Specifically, regarding cellulose doped PES composite membranes, it has been determined that degradation in TGA curves can exhibit a two-stage character with the addition of PES and cellulose, and that cellulose affects the composite degradation profile.

The WU_C, S_P, and D_C of the synthesized membranes for fuel cell applications were investigated at 25ºC and 80ºC, and the results are given in Figure 5. The WU_C value for pristine PES is 5.34, this value increases to 5.68 in the membrane with 1% cellulose doped, and reaches the highest value among the synthesized membranes, 7.91, in the PES-5% Cellulose membrane (Figure 5a). Similarly, the S_P (1.94) and D_C (1.45) values are also maximum in the PES-5% Cellulose membrane. This increasing trend can be explained by the -OH groups on the surface of cellulose strengthen the membrane water interaction, increasing hydrophilization and water uptake (Nazri et al., 2021; Acarer Arat, 2026). The addition of cellulose to PES increased wettability and influenced membrane morphology through –OH induced hydrophilization and changes in the drying behavior of the casting solution. In contrast, the decrease in WUC to 2.16 and SP to 0.83 in the 10% cellulose composite suggests that as the doping ratio increases, the viscosity of the dope solution increases, slowing its diffusion and hindering water uptake, leading to more compact structures and reduced pore connection. Furthermore, under high loading, agglomerated particles can create structural heterogeneity. These two effects resulted in a decrease in WUC and SP, with less accessible hydrophilic surface and lower effective porosity.
As the temperature increases, the WUC in pristine PES rises to 5.91, it reaches a maximum of 7.32 ± 0.89 in PES-%1 Cellulose and 9.97 ± 0.64 in PES-%5 Cellulose. Similarly, at 25°C, the WU_C remains at 3.09 in 10% cellulose (Figure 5b). S_P and D_C values are also highest in 5% cellulose (S=1.98 ± 0.45, D=1.53 ± 0.20). The increase in water uptake and swelling with increasing temperature, due to reasons such as increased polymer chain mobility and water diffusion, is a behavior commonly observed in the ion exchange/proton transport membrane (Palanisamy et al., 2023; Abouricha et al., 2024). In this context, it was determined that cellulose significantly increases membrane hydration at 80°C, but water uptake remains limited "even at high temperatures" with a 10% load. This is consistent with viscosity-induced structural compaction and/or the reduction of the accessible -OH area by agglomerate additive. PES-5% cellulose provides the highest hydration by increasing WUC, SP, and DC at both 25°C and 80°C. This is an advantageous aspect for proton transport in PEM applications. The lower WU_C and S_P of PES-10% cellulose are positive in terms of dimensional stability and may be associated with a more compact structure and/or increased heterogeneity due to agglomeration. The effect of this structural change on proton-transport behavior is discussed in the EIS section.

Mechanical strength tests were performed on the membranes for fuel cell applications. The tensile strength and elongation at break values of the membranes resulting from the mechanical strength tests are given in Figure 6. Tensile test results show that cellulose doped increases the maximum stress that membranes can withstand while reducing elongation at break. While pristine PES had a tensile strength of 48.3 MPa and elongation at break of 27.8%, with 1% cellulose, the strength increased to 50.1 MPa and elongation decreased to 24.9%. The most significant improvement was observed with 5% cellulose (tensile strength 58.7 MPa), but elongation decreased to 20.2%. When the cellulose content increased to 10%, the strength decreased to 53.6 MPa, while elongation remained at 19.7%. The main reason for the increase in strength is that cellulose acts as a rigid doped phase, facilitating load transfer to the polymer matrix. The high mechanical modulus and strength of cellulose, along with the strong fiber-matrix interactions stemming from hydrogen bonds, are the main mechanisms supporting efficient stress transfer in composites (Rafieian et al., 2020; Grzybek et al., 2024). Furthermore, it was determined that hydrogen bond interactions can occur between the polar functional groups of PES and the -OH groups of cellulose, strengthening intercomponent adhesion.
The regular decrease in elongation at fracture is consistent with the cellulose addition restricting PES chain mobility and creating a more rigid behavior in the composite structure. Specifically, the crystalline regions of cellulose reduce the elastic deformation capacity within the matrix. This is consistent with XRD pattern, and elongation capacity decreases as the crystalline structure increases. The decrease in tensile strength at 10% cellulose compared to 5% is due to agglomeration and structural inhomogeneity under excessive filler loading, as frequently observed in the literature (Alasfar et al., 2022; Grzybek et al., 2024). Excessive addition of the filler material leads to large voids and irregular pore morphology, weakening mechanical properties. This is fundamentally due to agglomeration of the filler material and

weakened interfacial adhesion. The heterogeneous distribution, particle clusters, and particle size distribution seen in SEM images under high loading facilitate crack initiation and reduce strength .

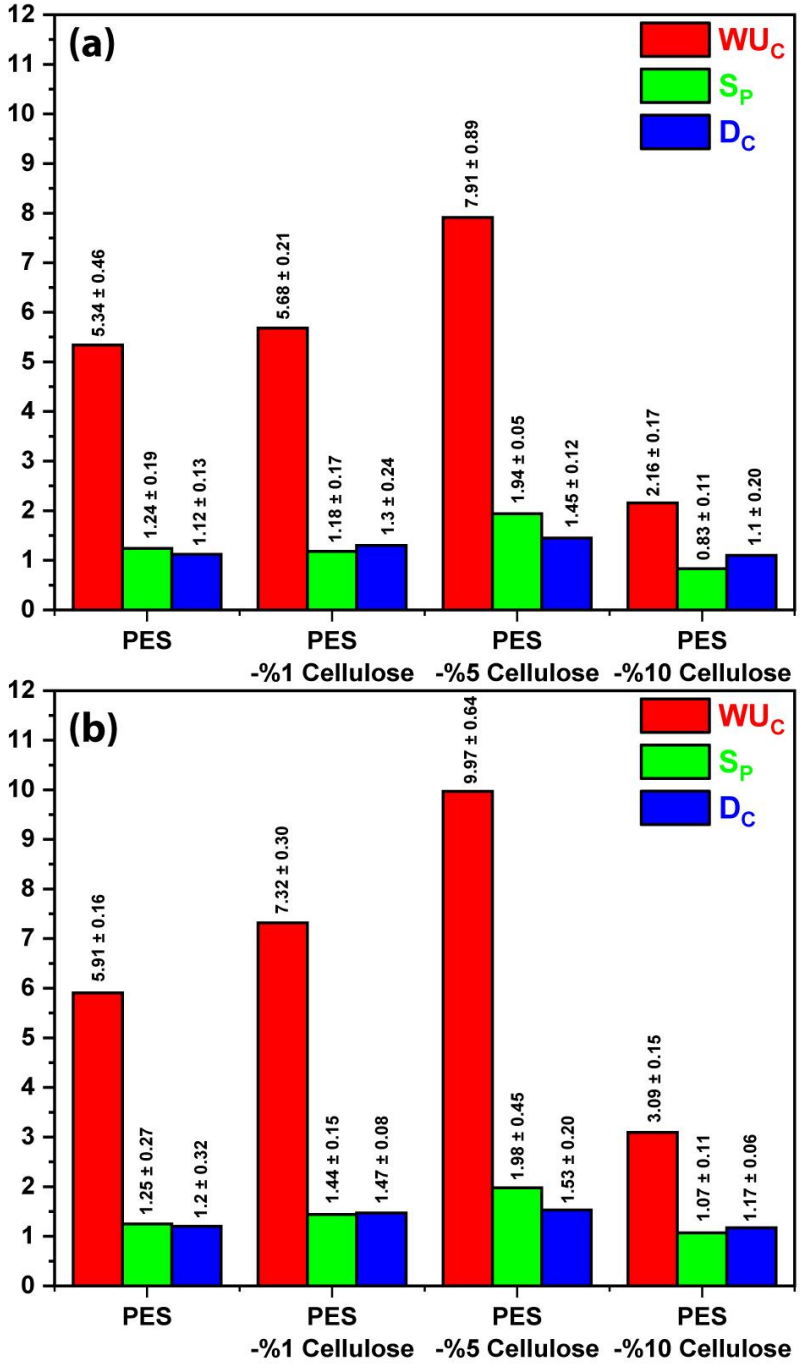

Figure 5. WU_C, S_P, and D_C values of the synthesized membranes at a) 25°C and b) 80°C.

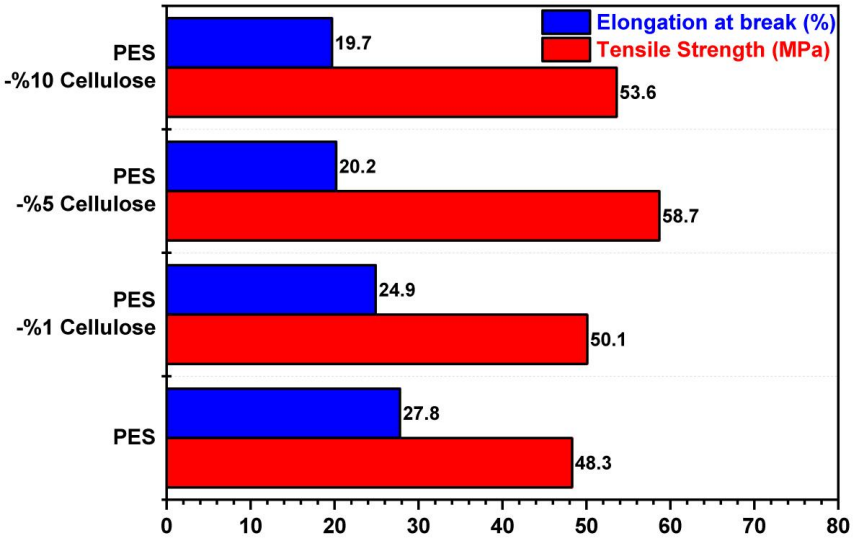

Figure 6. Mechanical strength results of synthesized membranes.

IEC experiments, conducted to determine the ion-exchange groups of the membranes, were performed using the titration method, and the results obtained are given in Figure 7.

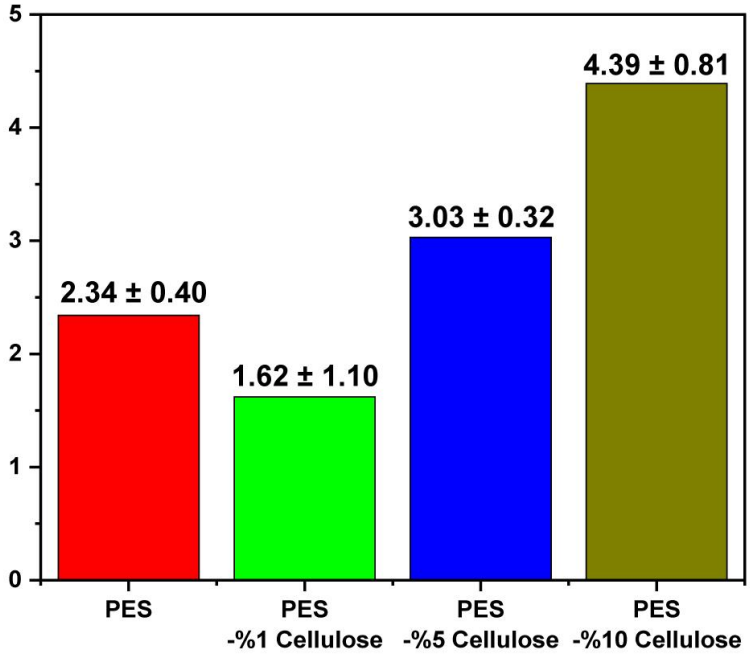

Figure 7. IEC values of synthesized membranes.

It was determined that the IEC increased significantly when the cellulose content reached 5% and 10%, but decreased at the 1% compared to pristine PES. The increase in IEC can be associated with either greater accessibility of titratable sites or a stronger ion-exchange response under the applied pretreatment and titration conditions. Therefore, the increased IEC at 5%-10% cellulose content indicates a clear increase in acidic centers in the composite (Komers et al., 2025). Since the -OH groups of cellulose alone are not fixed ion exchange groups and the PES backbone was not sulfonated in this study, the increase in IEC with 5% and especially 10% cellulose is more cautiously attributed to changes in membrane hydration, acid uptake, and the accessibility of titratable sites within the composite structure. The decrease in IEC from 2.34 ± 0.40 to 1.62 ± 1.10 at 1% cellulose is thought to be due to the accessibility effect. That is, even though hydrophilization increases, it does not increase the number of stable acidic groups but rather covers some of the accessible protonable centers in the matrix (Zhang

et al., 2011). IEC depends not only on the density of chemical groups but also on the accessibility of these groups for ion exchange. The fact that the IEC was highest at 10% cellulose (4.39 ± 0.81 meq g^{-1}) is a significant finding, but when interpreting this in terms of performance, it should be considered in conjunction with WU_C and S_P results. A higher IEC is often associated with higher water uptake and greater swelling. This can increase proton conductivity in some cases, but at extreme values, it can negatively affect dimensional stability and mechanical strength.

Impedance analyses were performed to determine the proton conductivity of the membranes, and the resulting Nyquist diagram is given in Figure 8.

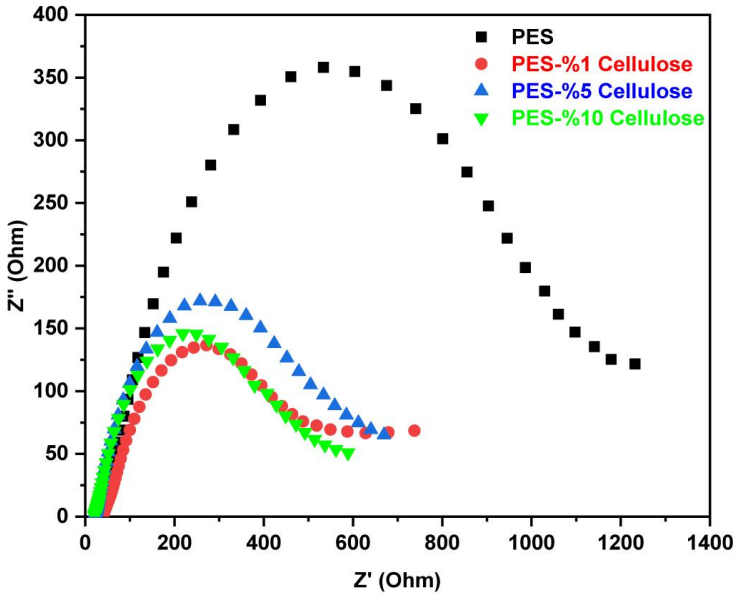

Figure 8. Nyquist diagram obtained from impedance analysis of synthesized membranes.

Nyquist diagrams clearly show that cellulose addition significantly reduced the proton transport resistance of PES membranes. For a clearer interpretation of the impedance response, the principal semicircle of the Nyquist plots was fitted with the equivalent circuit R_s-(R1||CPE1), where R_s denotes the initial cutoff point and R1 denotes the arc width. The extracted fitting parameters are summarized in Table 1. According to the equivalent-circuit fitting, the R_s values were 40.74 Ω, 23.18 Ω, 43.24 Ω, and 23.30 Ω for pristine PES and the membranes containing 1 wt%, 5 wt%, and 10 wt% cellulose, respectively, whereas the arc widths (R1) decreased from 1052 Ω for pristine PES to 519 Ω, 460 Ω, and 435 Ω, respectively. In parallel, the increase in proton conductivity from 2.73 mS cm^{-1} (PES) to the range of 12.8-14.8 mS cm^{-1} indicates that cellulose strengthens conductive pathways favorable for proton transport within the PES matrix. This improvement, when considered together with the WU_C, S_P, mechanical, and IEC results, suggests that proton transport in these membranes is governed not only by the total amount of absorbed water, but also by the effectiveness of hydrated transport pathways within the composite structure. Accordingly, although the 5% cellulose membrane showed the highest bulk water uptake, the 10% cellulose membrane may have provided more effective local proton-conduction pathways under the measurement conditions, which resulted in the lowest fitted arc width and the lowest membrane-related resistance (Shah & Hakim, 2025). This behavior may be related to more effective local proton-conduction pathways, hydrogen bond assisted transport, and the higher apparent ion-exchange response observed for the 10% cellulose membrane. Indeed, it is particularly emphasized that proton conduction in cellulosic materials is strongly dependent on the presence of water, and hydrated systems are critical. The fact that the IEC results progress in the same direction as the decrease in bulk resistance in EIS suggests that not only water uptake but also the density of accessible proton centers has increased. In particular, the proton conductivity has been significantly increased thanks to the formation of a network via hydrogen bonding in the cellulose phase containing acidic groups/enhanced ionic character in the composite (Wei et al., 2016).

Table 1. Parameters obtained from Nyquist plots of the synthesized membranes.

Membrane	R_s	R1	CPE-T (Q) ($x10^4$)	CPE-P (n)
PES	40.74	1052	1.39	0.75
PES- %1 Cellulose	23.18	519	2.79	0.76
PES- %5 Cellulose	43.24	460	3.22	0.67
PES- %10 Cellulose	23.30	435	2.80	0.76

To facilitate a more understandable interpretation of the results obtained from this study, the values obtained from fuel cell tests are presented in Table 2 in comparison with the literature.

Table 2. Comparison of PEMs reported in the literature and in this study.

Membrane	Water Uptake (%)	Swelling (%)	Tensile Strength, MPa	Proton Conductivity, mS/cm^{-1}	Measurement Conditions
Nafion 117 (S. Thangarasu & T. H. Oh, 2022)	40	16.5	NR	95	80°C
SFPEEKK-60/4% CNC (Ni et al., 2018)	115.73	32.6	NR	245	90°C
SPEEK/SEC composite (Charradi et al., 2023)	30	NR	NR	110	Above 100°C
SPEEK/MCC composite (Moussa et al., 2024)	92	NR	NR	186	110°C
Modified bacterial cellulose/APTES membrane (Yang et al., 2024)	56	39	86	62.2	WU/SR at 45°C; conductivity at 95°C
PES-%1 Cellulose (This work)	9.97	1.98	58.7	14.8	WU/SR at 80°C; conductivity at 30°C

As summarized in Table 2, cellulose-containing proton exchange membranes reported in the literature generally improve hydration-assisted proton transport, although the extent of improvement strongly depends on the polymer matrix, cellulose derivative, and testing conditions. SPEEK-based systems containing cellulose-derived additives, such as CNC, SEC, or MCC, typically exhibit markedly higher proton conductivity than many non-sulfonated hydrocarbon membranes, often accompanied by increased water uptake and, in some cases, higher swelling. In contrast, the present PES/cellulose membranes showed a more moderate conductivity level, with a maximum of 14.8 mS/cm, but provided comparatively strong mechanical performance, reaching 58.7 MPa in tensile strength. Furthermore, exhibiting this high conductivity at low temperatures is a very promising finding. This behavior indicates that the present fluorine-free PES/cellulose system offers a balanced combination of transport and mechanical integrity, even though its conductivity remains below that of highly sulfonated SPEEK-based counterparts and commercial Nafion-type benchmarks.

4. Discussion and Conclusion

This study is based on an approach to recover cellulose from waste newsprint and produce composite PEM candidates by solution casting and incorporating this bio-based phase into a PES matrix in the range of 1-10 wt%. The main rationale for this study is to explore more sustainable hydrocarbon-based membrane candidates with high film forming capability that may help address some limitations associated with Nafion-based systems, such as cost and humidity-sensitive conductivity. FTIR and XRD findings of the cellulose show that the cellulosic backbone is preserved and the traces of crystalline "ash/filler" that may come from fillers/inorganic additives in newsprint are significantly reduced. In particular, the absence of prominent calcite reflections within the cellulose pattern supports the purity of the cellulose. While the amorphous character of PES is preserved in the composite, the appearance of cellulose reflections in a shoulder shape around 15-17^{o} and 22-23^{o} in 10% cellulose indicates that the cellulose is present in the matrix without completely losing its crystalline areas. In contrast, the weakening and broadening of the peaks suggests a decrease in the crystalline area/arrangement within the polymer. In terms of performance, the -OH-rich/hydrophilic structure of cellulose strengthened the membrane-water interaction, increasing the tendency for water uptake and swelling at 25-80^{o}C. The highest hydration was obtained for the 5% cellulose membrane, consistent with the hydrophilic role of cellulose and its contribution to water-membrane interactions. The limitations of WU_C and S_P in the 10% cellulose membrane were attributed to increased solution viscosity, which may promote a more compact structure or heterogeneity due to agglomeration. However, this did not prevent the formation of effective proton-transport pathways under the EIS measurement conditions. This is also supported by the observation of increased roughness/heterogeneity and fibril-derived irregularities in some regions on the 10% cellulose surface in the SEM. However, the EIS results showed that the highest proton conductivity was obtained for the 10% cellulose membrane, even though the highest WUC, SP, and mechanical strength were observed at 5% cellulose. This indicates that proton transport in these membranes was not governed solely by the total amount of absorbed water, but also by the effectiveness and continuity of hydrated proton-transport pathways within the composite structure. Accordingly, while the 5% cellulose membrane provided the best overall balance between hydration and mechanical integrity, the 10% cellulose membrane exhibited the highest conductivity under the applied measurement conditions.

In conclusion, cellulose obtained from waste paper improved the hydration-related and transport-related properties of PES membranes; however, at higher loading, the system tended toward structural compaction and agglomeration-related heterogeneity. From a single-property perspective, the highest proton conductivity was obtained for the 10% cellulose membrane. However, considering hydration, dimensional behavior, and mechanical strength together, the 5% cellulose membrane provided the most balanced overall performance. Thus, the optimum cellulose loading depends on the target property. 10% cellulose yielded the highest conductivity, whereas 5% cellulose offered the best overall balance of properties.

Acknowledgments / Funding

This study was partially supported by the Scientific and Technological Research Council of Türkiye (TÜBİTAK) under the 2209-A Research Project Support Programme for Undergraduate Students.

Authors' Contributions

Nisa Doğa Erdemir: Conceptualization, Formal Analysis, Investigation, Experimental study; **Çağla Can:** Conceptualization, Formal Analysis, Investigation, Experimental study; **Yavuz Yağızatlı:** Writing -Review & Editing, Data Analysis, Supervision.

Declaration of Competing Interests

There are no conflicts of interest in this work.

Statement on Research and Publication Ethics

The authors of this article declare that the materials and methods used in this study did not require approval from an ethics committee

Ethics Committee Statement

The author(s) declare that the materials and methods used in this study do not require ethics committee approval and/or any legal or special permission.

Use of Artificial Intelligence

The author(s) declare that no generative artificial intelligence was used in the writing of this manuscript or in the creation of figures, graphs, tables, or their corresponding captions.

References

Abouricha, S., Aziam, H., Noukrati, H., Sel, O., Saadoune, I., Lahcini, M., & Youcef, H. B. (2024). Biopolymers-based proton exchange membranes for fuel cell applications: A comprehensive review. *ChemElectroChem*, 11(9), e202300648. https://doi.org/10.1002/celc.202300648

Acarer Arat, S. (2026). Improvement of water flux, treatment efficiency, and fouling resistance of polyethersulfone/cellulose acetate blend ultrafiltration membranes using nanomaterials derived from renewable resources. *Pamukkale University Journal of Engineering Sciences*, 32(4), 0-0. https://doi.org/10.65206/pajes.70729

Adeniyi, A., Odo, G. O., Gonzalez-Ortiz, D., Pochat-Bohatier, C., Mbakop, S., & Onyango, M. S. (2023). A comparison of the effect of cellulose nanocrystals (cncs) and polyethylene glycol (peg) as additives in ultrafiltration membranes (pes-uf): Characterization and performance. Polymers (Basel), 15(12). https://doi.org/10.3390/polym15122636

Ahmad, M. S., Mohshim, D. F., Nasir, R., Mannan, H. A., & Mukhtar, H. (2018). Effect of solvents on the morphology and performance of polyethersulfone (pes) polymeric membranes material for co2/ch4 separation. IOP Conference Series: Materials Science and Engineering, 290(1), 012074. https://doi.org/10.1088/1757-899X/290/1/012074

Alasfar, R. H., Kochkodan, V., Ahzi, S., Barth, N., & Koç, M. (2022). Preparation and characterization of polysulfone membranes reinforced with cellulose nanofibers. *Polymers*, 14(16), 3317. https://doi.org/10.3390/polym14163317

Chambre, D. R., & Dochia, M. (2021). Ft-ir characterization of cellulose crystallinity from raw bast fibers. Scientific and Technical Bulletin, Series: Chemistry, Food Science and Engineering, 18, 10-17. https://doi.org/10.12982/CMJS.2019.043

Charradi, K., Landolsi, Z., Gabriel, L., Mabrouk, W., Koschella, A., Ahmed, Z., Elnaggar, A., Heinze, T., & Keshk, S. M. A. S. (2023). Incorporating of sulfo ethyl cellulose to augment the performance of sulfonated poly (ether ether ketone) composite for proton exchange membrane fuel cells. *Journal of Solid State Electrochemistry*, 27(12), 3415-3423. https://doi.org/10.1007/s10008-023-05629-0

Council, N. R. (2006). Proceedings of a workshop to review path strategy, operating plan, and performance measures. https://doi.org/10.17226/11577

Dattilo, S., Puglisi, C., Mirabella, E. F., Spina, A., Scamporrino, A. A., Zampino, D. C., Blanco, I., Cicala, G., Ognibene, G., Di Mauro, C., & Samperi, F. (2020). Thermal degradation processes of aromatic poly(ether sulfone) random copolymers bearing pendant carboxyl groups. *Polymers* (Basel), 12(8). https://doi.org/10.3390/polym12081810

Daud, S. M., Kim, B. H., Ghasemi, M., & Daud, W. R. W. (2015). Separators used in microbial electrochemical technologies: Current status and future prospects. *Bioresource Technology*, 195, 170-179. https://doi.org/10.1016/j.biortech.2015.06.105

Di Virgilio, M., Basso Peressut, A., Arosio, V., Arrigoni, A., Latorrata, S., & Dotelli, G. (2023). Functional and environmental performances of novel electrolytic membranes for pem fuel cells:

A lab-scale case study. *Clean Technologies*, 5(1), 74-93. https://doi.org/10.3390/cleantechnol5010005

Etale, A., Onyianta, A. J., Turner, S. R., & Eichhorn, S. J. (2023). Cellulose: A review of water interactions, applications in composites, and water treatment. *Chemical Reviews*, 123(5), 2016-2048. https://doi.org/10.1021/acs.chemrev.2c00477

Golubenko, D. V., Korchagin, O. V., Voropaeva, D. Y., Bogdanovskaya, V. A., & Yaroslavtsev, A. B. (2022). Membranes based on polyvinylidene fluoride and radiation-grafted sulfonated polystyrene and their performance in proton-exchange membrane fuel cells. *Polymers*, 14(18), 3833. https://doi.org/10.3390/polym14183833

Grzybek, P., Dudek, G., & van der Bruggen, B. (2024). Cellulose-based films and membranes: A comprehensive review on preparation and applications. *Chemical Engineering Journal*, 495, 153500. https://doi.org/10.1016/j.cej.2024.153500

He, Y., Miao, J., Chen, S., Zhang, R., Zhang, L., Tang, H., & Yang, H. (2019). Preparation and characterization of a novel positively charged composite hollow fiber nanofiltration membrane based on chitosan lactate. RSC advances, 9(8), 4361-4369. https://doi.org/10.1039/C8RA09855G

Hossain Bhuiyan, M. M., & Siddique, Z. (2025). Hydrogen as an alternative fuel: A comprehensive review of challenges and opportunities in production, storage, and transportation. *International Journal of Hydrogen Energy*, 102, 1026-1044. https://doi.org/10.1016/j.ijhydene.2025.01.033

Huang, C. K., & Kerr, P. F. (1960). Infrared study of the carbonate minerals. *American Mineralogist*, 45(3-4), 311-324.

Jahani, Z., Mosaffa, E., Oroujzadeh, M., & Ghafuri, H. (2023). Performance evaluation of polyethersulfone membranes modified with poly (acrylic acid-co-n-vinyl pyrrolidone) grafted mesoporous carbon nitride for effective removal of cadmium(ii) from wastewater. *Polymers for Advanced Technologies*, 34(12), 3803-3817. https://doi.org/10.1002/pat.6183

Justin Jose Sheela, A. S., Moorthy, S., Maria Mahimai, B., Sekar, K., Kannaiyan, D., & Deivanayagam, P. (2023). Sulfonated poly ether sulfone membrane reinforced with bismuth-based organic and inorganic additives for fuel cells. *ACS Omega*, 8(30), 27510-27518. https://doi.org/10.1021/acsomega.3c03143

Koloti, L. E., Gule, N. P., Arotiba, O. A., & Malinga, S. P. (2018). Laccase-immobilized dendritic nanofibrous membranes as a novel approach towards the removal of bisphenol a. Environmental Technology, 39(3), 392-404. https://doi.org/10.1080/09593330.2017.1301570

Komers, F., Plachá, D., Van der Bruggen, B., & Velizarov, S. (2025). Towards sustainable proton exchange membranes: Materials and challenges for water electrolysis. *Water*, 17(22), 3297. https://doi.org/10.3390/w17223297

Kumar, A., Negi, Y. S., Choudhary, V., & Bhardwaj, N. K. (2014). Characterization of cellulose nanocrystals produced by acid-hydrolysis from sugarcane bagasse as agro-waste journal of materials physics and chemistry 2: 1–8. no. 1 (2014), 1-8. https://doi.org/10.12691/jmpc-2-1-1

Luhar, I., Luhar, S., Abdullah, M. M., Nabiałek, M., Sandu, A. V., Szmidla, J., Jurczyńska, A., Razak, R. A., Aziz, I. H., Jamil, N. H., & Deraman, L. M. (2021). Assessment of the suitability of ceramic waste in geopolymer composites: *An appraisal. Materials*, 14(12), 3279. https://doi.org/10.3390/ma14123279

Madheswaran, D. K., Thangavelu, P., Krishna, R., Thangamuthu, M., Joseph Chandran, A., & Colak, I. (2023). Carbon-based materials in proton exchange membrane fuel cells: A critical review on performance and application. *Carbon Letters*, 33(6), 1495-1518. https://doi.org/10.1007/s42823-023-00526-y

Moussa, M. A. B., Ahmed, Z., Charradi, K., Fraj, B. B., Boufi, S., Koschella, A., Heinze, T., Keshk, S. M. A. S., & Assaker, I. B. (2024). Performance of high sulfonated poly(ether ether ketone) improved with microcrystalline cellulose and 2,3-dialdehyde cellulose for proton exchange membranes. *Materials for Renewable and Sustainable Energy*, 13(3), 319-331. https://doi.org/10.1007/s40243-024-00267-6

Nazri, A. I., Ahmad, A. L., & Hussin, M. H. (2021). Microcrystalline cellulose-blended polyethersulfone membranes for enhanced water permeability and humic acid removal. *Membranes*, 11(9), 660. https://doi.org/10.3390/membranes11090660

Nazri, A. I., Ahmad, A. L., & Hussin, M. H. (2021). Microcrystalline cellulose-blended polyethersulfone membranes for enhanced water permeability and humic acid removal. Membranes (Basel), 11(9). https://doi.org/10.3390/membranes11090660

Ni, C., Wei, Y., Zhao, Q., Liu, B., Sun, Z., Gu, Y., Zhang, M., & Hu, W. (2018). Novel proton exchange membranes based on structure-optimized poly(ether ether ketone ketone)s and nanocrystalline cellulose. *Applied Surface Science*, 434, 163-175. https://doi.org/10.1016/j.apsusc.2017.09.094

Nong, D., Simshauser, P., & Nguyen, D. B. (2021). Greenhouse gas emissions vs co2 emissions: Comparative analysis of a global carbon tax. *Applied Energy*, 298, 117223. https://doi.org/10.1016/j.apenergy.2021.117223

Nurazzi, N. M., Asyraf, M. R. M., Rayung, M., Norrrahim, M. N. F., Shazleen, S. S., Rani, M. S. A., Shafi, A. R., Aisyah, H. A., Radzi, M. H. M., Sabaruddin, F. A., Ilyas, R. A., Zainudin, E. S., & Abdan, K. (2021). Thermogravimetric analysis properties of cellulosic natural fiber polymer composites: A review on influence of chemical treatments. Polymers (Basel), 13(16). https://doi.org/10.3390/polym13162710

Oh, K. H., Ko, Y.-H., & Kim, K.-J. (2020). Mechanical properties of amorphous pei, pes, and pvc up to 11 gpa studied by brillouin light scattering. *Physica B: Condensed Matter*, 576, 411722. https://doi.org/10.1016/j.physb.2019.411722

Oprică, G. M., Panaitescu, D. M., Usurelu, C. D., Vlăsceanu, G. M., Stanescu, P. O., Lixandru, B. E., Vasile, V., Gabor, A. R., Nicolae, C.-A., Ghiurea, M., & Frone, A. N. (2023). Nanocellulose sponges containing antibacterial basil extract. *International Journal of Molecular Sciences*, 24(14), 11871. https://doi.org/10.3390/ijms241411871

Pagacz, J., Naglik, B., Stach, P., Drzewicz, P., & Natkaniec-Nowak, L. (2020). Maturation process of natural resins recorded in their thermal properties. *Journal of Materials Science*, 55(10), 4504-4523. https://doi.org/10.1007/s10853-019-04302-0

Palanisamy, G., Oh, T. H., & Thangarasu, S. (2023). Modified cellulose proton-exchange membranes for direct methanol fuel cells. Polymers, 15(3), 659. https://doi.org/10.3390/polym15030659

Pervez, M. N., Talukder, M. E., Mishu, M. R., Buonerba, A., Del Gaudio, P., Stylios, G. K., Hasan, S. W., Zhao, Y., Cai, Y., Figoli, A., Zarra, T., Belgiorno, V., Song, H., & Naddeo, V. (2022). One-step fabrication of novel polyethersulfone-based composite electrospun nanofiber membranes for food industry wastewater treatment. *Membranes*, 12(4), 413. https://doi.org/10.3390/membranes12040413

Phogat, P., Chand, B., Shreya, Jha, R., & Singh, S. (2025). Hydrogen and methanol fuel cells: A comprehensive analysis of challenges, advances, and future prospects in clean energy. International *Journal of Hydrogen Energy*, 109, 465-485. https://doi.org/10.1016/j.ijhydene.2025.02.133

Plermjai, K., Boonyarattanakalin, K., Mekprasart, W., Phoohinkong, W., Pavasupree, S., & Pecharapa, W. (2019). Optical absorption and ftir study of cellulose/tio2 hybrid composites. *Chiang Mai Journal of Science*, 46(3), 618-625. https://doi.org/10.12982/CMJS.2019.043

Poongan, A., Kesava, M., Mandal, A., & Murugan, E. (2023). Effect of zro2 nanoparticles on phosphoric acid-doped poly (ethylene imine)/polyvinyl alcohol) membrane for medium-temperature polymer electrolyte membrane fuel cell applications. *International Journal of Hydrogen Energy*, 48(70), 27371-27382. https://doi.org/10.1016/j.ijhydene.2023.03.418

Qu, P., Tang, H., Gao, Y., Zhang, L.-p., & Wang, S. (2010). Polyethersulfone composite membrane blended with cellulose fibrils. *BioResources*, 5(4), 2323-2336. https://doi.org/10.15376/biores.5.4.2323-2336

Rafieian, F., Mousavi, M., Dufresne, A., & Yu, Q. (2020). Polyethersulfone membrane embedded with amine functionalized microcrystalline cellulose. *International Journal of Biological Macromolecules*, 164, 4444-4454. https://doi.org/10.1016/j.ijbiomac.2020.09.017

Rantuch, P., & Chrebet, T. (2014). Thermal decomposition of cellulose insulation. *Cellul. Chem. Technol*, 48(5), 461-467.

Samaniego, A. J., & Espiritu, R. (2022). Prospects on utilization of biopolymer materials for ion exchange membranes in fuel cells. *Green Chemistry Letters and Reviews*, 15(1), 253-275. https://doi.org/10.1080/17518253.2022.2040599

Sanchez, J. Y., Iojoiu, C., Alloin, F., Guindet, J., & Leprêtre, J. C. (2009). Fuel cells – proton-exchange membrane fuel cells | membranes: Non-fluorinated. In J. Garche (Ed.), Encyclopedia of

electrochemical power sources (pp. 700-715). Elsevier. https://doi.org/10.1016/B978-044452745-5.00887-X

Sandoval-Olvera, I. G., Villafaña-López, L., Reyes-Aguilera, J. A., Ávila-Rodríguez, M., Razo-Lazcano, T. A., & González-Muñoz, M. P. (2017). Surface modification of polyethersulfone membranes with goethite through self-assembly. *Desalination and Water Treatment*, 65, 199-207. https://doi.org/10.5004/dwt.2017.20302

Seddiqi, H., Oliaei, E., Honarkar, H., Jin, J., Geonzon, L. C., Bacabac, R. G., & Klein-Nulend, J. (2021). Cellulose and its derivatives: Towards biomedical applications. *Cellulose*, 28(4), 1893-1931. https://doi.org/10.1007/s10570-020-03674-w

Selim, A., Szijjártó, G. P., Románszki, L., & Tompos, A. (2022). Development of wo(3)-nafion based membranes for enabling higher water retention at low humidity and enhancing pemfc performance at intermediate temperature operation. Polymers (Basel), 14(12). https://doi.org/10.3390/polym14122492

Shah, M., & Hakim, N. U. D. (2025). Advances in nanocellulose proton conductivity and applications in polymer electrolyte membrane fuel cells. *Next Materials*, 6, 100484. https://doi.org/10.1016/j.nxmate.2025.100484

Spiridigliozzi, L. (2018). Fuel cells. In L. Spiridigliozzi (Ed.), Doped-ceria electrolytes: Synthesis, sintering and characterization (pp. 3-13). Springer International Publishing. https://doi.org/10.1007/978-3-319-99395-9_2

Teixeira, F. C., Teixeira, A. P. S., & Rangel, C. M. (2023). Chemical stability of new nafion membranes doped with bisphosphonic acids under fenton oxidative conditions. *International Journal of Hydrogen Energy*, 48(96), 37489-37499. https://doi.org/10.1016/j.ijhydene.2023.04.063

Teixeira, F. C., Teixeira, A. P. S., & Rangel, C. M. (2025). New modified speek-based proton exchange membranes. *Polymers*, 17(12), 1646. https://doi.org/10.3390/polym17121646

Tellez-Cruz, M. M., Escorihuela, J., Solorza-Feria, O., & Compañ, V. (2021). Proton exchange membrane fuel cells (pemfcs): Advances and challenges. *Polymers*, 13(18), 3064. https://doi.org/10.3390/polym13183064

Thangarasu, S., & Oh, T.-H. (2022). Recent developments on bioinspired cellulose containing polymer nanocomposite cation and anion exchange membranes for fuel cells (pemfc and afc). *Polymers*, 14(23), 5248. https://doi.org/10.3390/polym14235248

Tintner, J., Reiter, F., Smidt, E., & Hinterstoisser, B. (2018). Aging of newspaper since 1959 under archive conditions—a quantification of different effects using ft-ir spectroscopy. *Cell. Chem. Technol*, 52, 105-111. https://doi.org/10.3390/molecules23010105

Treekamol, Y., Schieda, M., Robitaille, L., MacKinnon, S. M., Mokrini, A., Shi, Z., Holdcroft, S., Schulte, K., & Nunes, S. P. (2014). Nafion®/odf-silica composite membranes for medium temperature proton exchange membrane fuel cells. *Journal of Power Sources*, 246, 950-959. https://doi.org/10.1016/j.jpowsour.2013.01.178

Vârban, R., Crișan, I., Vârban, D., Ona, A., Olar, L., Stoie, A., & Ștefan, R. (2021). Comparative ft-ir prospecting for cellulose in stems of some fiber plants: Flax, velvet leaf, hemp and jute. *Applied Sciences*, 11(18), 8570. https://doi.org/10.3390/app11188570

Wang, H., Zhuang, X., Li, X., Wang, W., Wang, Y., & Cheng, B. (2015). Solution blown sulfonated poly(ether sulfone)/poly(ether sulfone) nanofiber-nafion composite membranes for proton exchange membrane fuel cells. *Journal of Applied Polymer Science*, 132(38). https://doi.org/10.1002/app.42572

Wang, X., Shi, L., Zhang, J., Cheng, J., & Wang, X. (2018). In situ formation of surface-functionalized ionic calcium carbonate nanoparticles with liquid-like behaviours and their electrical properties. *Royal Society Open Science*, 5(1), 170732. https://doi.org/10.1098/rsos.170732

Wei, Y., Li, X., Hu, Q., Ni, C., Liu, B., Zhang, M., Zhang, H., & Hu, W. (2016). Sulfonated nanocrystal cellulose/sulfophenylated poly(ether ether ketone ketone) composites for proton exchange membranes. *RSC advances*, 6(69), 65072-65080. https://doi.org/10.1039/C6RA10711G

Woo, S. H., Lee, S. Y., Yoon, Y.-G., Rigacci, A., Woo, J.-J., Beauger, C., & Kim, H.-J. (2022). Functionalized nanoclays for improved properties of composite proton exchange membranes. *Journal of Power Sources*, 549, 232083. https://doi.org/10.1016/j.jpowsour.2022.232083

Yagizatli, Y., Ulas, B., Cali, A., Sahin, A., & Ar, I. (2020). Improved fuel cell properties of nano-tio2 doped poly(vinylidene fluoride) and phosphonated poly(vinyl alcohol) composite blend

membranes for pem fuel cells. *International Journal of Hydrogen Energy*, 45(60), 35130-35138. https://doi.org/10.1016/j.ijhydene.2020.02.197

Yang, H., Gao, C.-M., Liu, S.-H., Ji, S.-F., Chen, H.-Y., & Chen, J.-C. (2020). Improving the hydrophilicity of polyethersulfone membrane by the combination of grafting technology and reverse thermally induced phase separation method. *Journal of Applied Polymer Science*, 137(43), 49327. https://doi.org/10.1002/app.49327

Yang, X., Huang, L., Deng, Q., & Dong, W. (2024). A sustainable and eco-friendly membrane for pem fuel cells using bacterial cellulose. *Polymers*, 16(21), 3017. https://doi.org/10.3390/polym16213017

Yörük, Ö., Uysal, D., & Doğan, Ö. M. (2025). Carbon-assisted hydrogen production via electrolysis at intermediate temperatures: Impact of mineral composition, functional groups, and membrane effects on current density. *Fuel*, 380, 133268. https://doi.org/10.1016/j.fuel.2024.133268

Zhang, N., Zhang, G., Xu, D., Zhao, C., Ma, W., Li, H., Zhang, Y., Xu, S., Jiang, H., Sun, H., & Na, H. (2011). Cross-linked membranes based on sulfonated poly (ether ether ketone) (speek)/nafion for direct methanol fuel cells (dmfcs). *International Journal of Hydrogen Energy*, 36(17), 11025-11033. https://doi.org/10.1016/j.ijhydene.2011.05.158

Zhang, S., Yuan, H., Wang, C., Liu, X., & Lu, J. (2020). Antifouling performance enhancement of polyethersulfone ultrafiltration membrane through increasing charge-loading capacity over prussian blue nanoparticles. *Journal of Applied Polymer Science*, 137(45), 49410. https://doi.org/10.1002/app.49410

Zhou, T., Li, Y., Wang, W., He, L., Cai, L., & Zeng, C. (2019). Application of a novel pva-based proton exchange membrane modified by reactive black kn-b for low-temperature fuel cells. *International Journal of Electrochemical Science*, 14(9), 8514-8531. https://doi.org/10.20964/2019.09.16